

VOLGA 22.02.2023

Yarovova. A.

# JADES NIRSpec Spectroscopy of GN-z11: Lyman- $\alpha$ emission and possible enhanced nitrogen abundance in a $z = 10.60$ luminous galaxy

Andrew J. Bunker<sup>1,\*</sup>, Aayush Saxena<sup>1,2</sup>, Alex J. Cameron<sup>1</sup>, Chris J. Willott<sup>3</sup>, Emma Curtis-Lake<sup>4</sup>, Peter Jakobsen<sup>5,6</sup>, Stefano Carniani<sup>7</sup>, Renske Smit<sup>8</sup>, Roberto Maiolino<sup>9,10,2</sup>, Joris Witstok<sup>9,10</sup>, Mirko Curti<sup>9,10,11</sup>, Francesco D'Eugenio<sup>9,10</sup>, Gareth C. Jones<sup>1</sup>, Pierre Ferruit<sup>12</sup>, Santiago Arribas<sup>13</sup>, Stephane Charlot<sup>14</sup>, Jacopo Chevallard<sup>1</sup>, Giovanna Giardino<sup>15</sup>, Anna de Graaff<sup>16</sup>, Tobias J. Looser<sup>9,10</sup>, Nora Lützgendorf<sup>17</sup>, Michael V. Maseda<sup>18</sup>, Tim Rawle<sup>17</sup>, Hans-Walter Rix<sup>16</sup>, Bruno Rodríguez Del Pino<sup>13</sup>, Stacey Alberts<sup>19</sup>, Eiichi Egami<sup>19</sup>, Daniel J. Eisenstein<sup>20</sup>, Ryan Endsley<sup>21</sup>, Kevin Hainline<sup>19</sup>, Ryan Hausen<sup>22</sup>, Benjamin D. Johnson<sup>20</sup>, George Rieke<sup>19</sup>, Marcia Rieke<sup>19</sup>, Brant E. Robertson<sup>23</sup>, Irene Shivaiei<sup>19</sup>, Daniel P. Stark<sup>19</sup>, Fengwu Sun<sup>19</sup>, Sandro Tacchella<sup>9,10</sup>, Mengtao Tang<sup>19</sup>, Christina C. Williams<sup>24,19</sup>, Christopher N. A. Willmer<sup>19</sup>, William M. Baker<sup>9,10</sup>, Stefi Baum<sup>25</sup>, Rachana Bhatawdekar<sup>12,26</sup>, Rebecca Bowler<sup>27</sup>, Kristan Boyett<sup>28,29</sup>, Zuyi Chen<sup>19</sup>, Chiara Circosta<sup>12</sup>, Jakob M. Helton<sup>19</sup>, Zhiyuan Ji<sup>19</sup>, Jianwei Lyu<sup>19</sup>, Erica Nelson<sup>30</sup>, Eleonora Parlanti<sup>7</sup>, Michele Perna<sup>13</sup>, Lester Sandles<sup>9,10</sup>, Jan Scholtz<sup>9,10</sup>, Katherine A. Suess<sup>23,31</sup>, Michael W. Topping<sup>19</sup>, Hannah Übler<sup>9,10</sup>, Imaan E. B. Wallace<sup>1</sup>, and Lily Whitler<sup>19</sup>

*(Affiliations can be found after the references)*

# Previous Studies

- Before the launch of JWST, the most distant galaxy with a tentative but plausible spectroscopic redshift was GN-z11 (Oesch et al. 2016). This was first selected as a likely high redshift Lyman-break candidate through multi-colour imaging with HST (Oesch et al. 2015), and subsequent HST/WFC3 slitless grism spectroscopy revealed a possible Lyman break in the continuum (Oesch et al. 2016), yielding a redshift of  $z_{\text{grism}} = 11.09$
- With an apparent H160 magnitude of  $26.0 \pm 0.1$ , GN-z11 is remarkably bright, up to 3 times more luminous than the characteristic rest-UV luminosity ( $L^?$ ) measured from luminosity functions at  $z \sim 6 - 8$  (e.g. Finkelstein et al. 2015; Bouwens et al. 2015). Using Spitzer/IRAC fluxes, Oesch et al. (2016) estimated its stellar mass to be  $M^? = 10^9 M_{\odot}$ , indicating a rapid build up of stellar mass in the very early Universe.

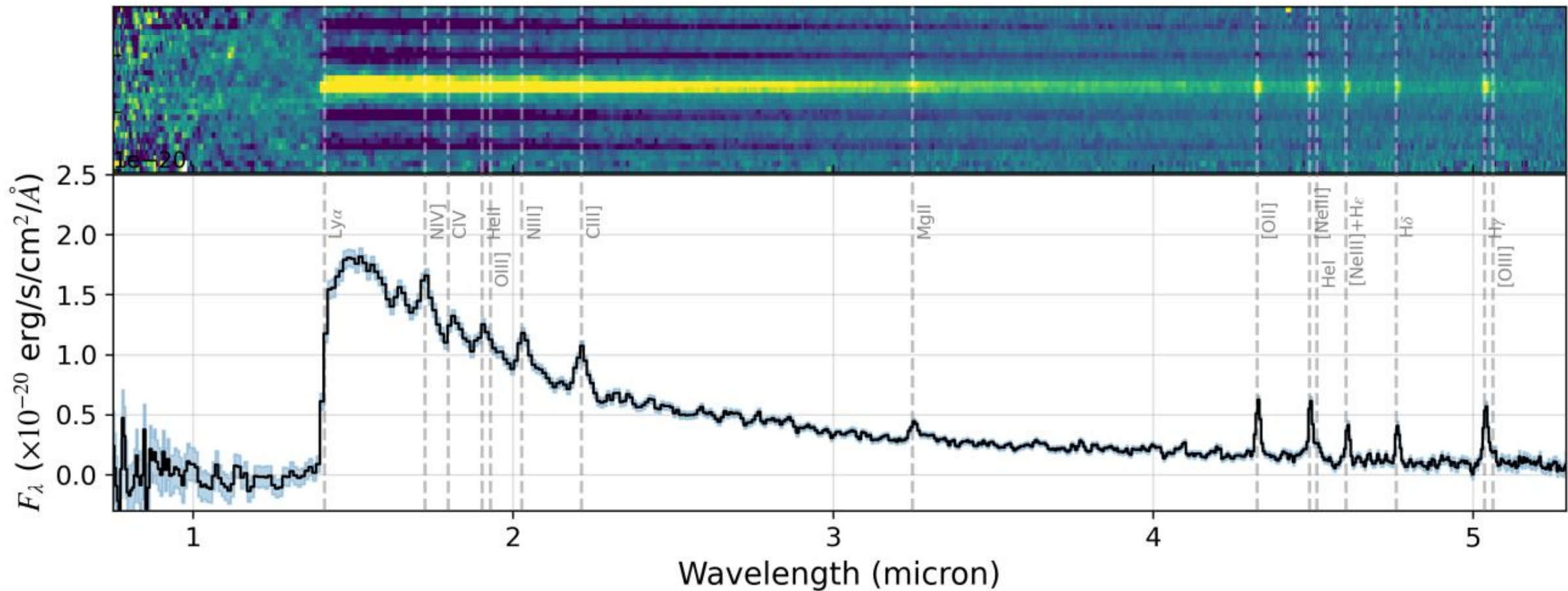


**Fig. 1.** 2D (top) and 1D (bottom) spectra of GN-z11 using PRISM/CLEAR configuration of NIRSpec. Prominent emission lines present in the spectra are marked. The signal to noise ratio (SNR) of the continuum is high and the emission lines are clearly seen in both the 1D and 2D spectra.

In this paper, we report an unambiguous spectroscopic redshift of  $z = 10.6034$  for GN-z11 using deep NIRSpec observations in the GOODS-North field via the robust detection of several emission lines including N iv]  $\lambda$  1486, N iii]  $\lambda\lambda$  1747, 1749, Ciii]  $\lambda\lambda$  1907, 1909, [O ii]  $\lambda\lambda$  3726, 3729, [Ne iii]  $\lambda\lambda$  3869, 3967, H  $\delta$  and H  $\gamma$ .

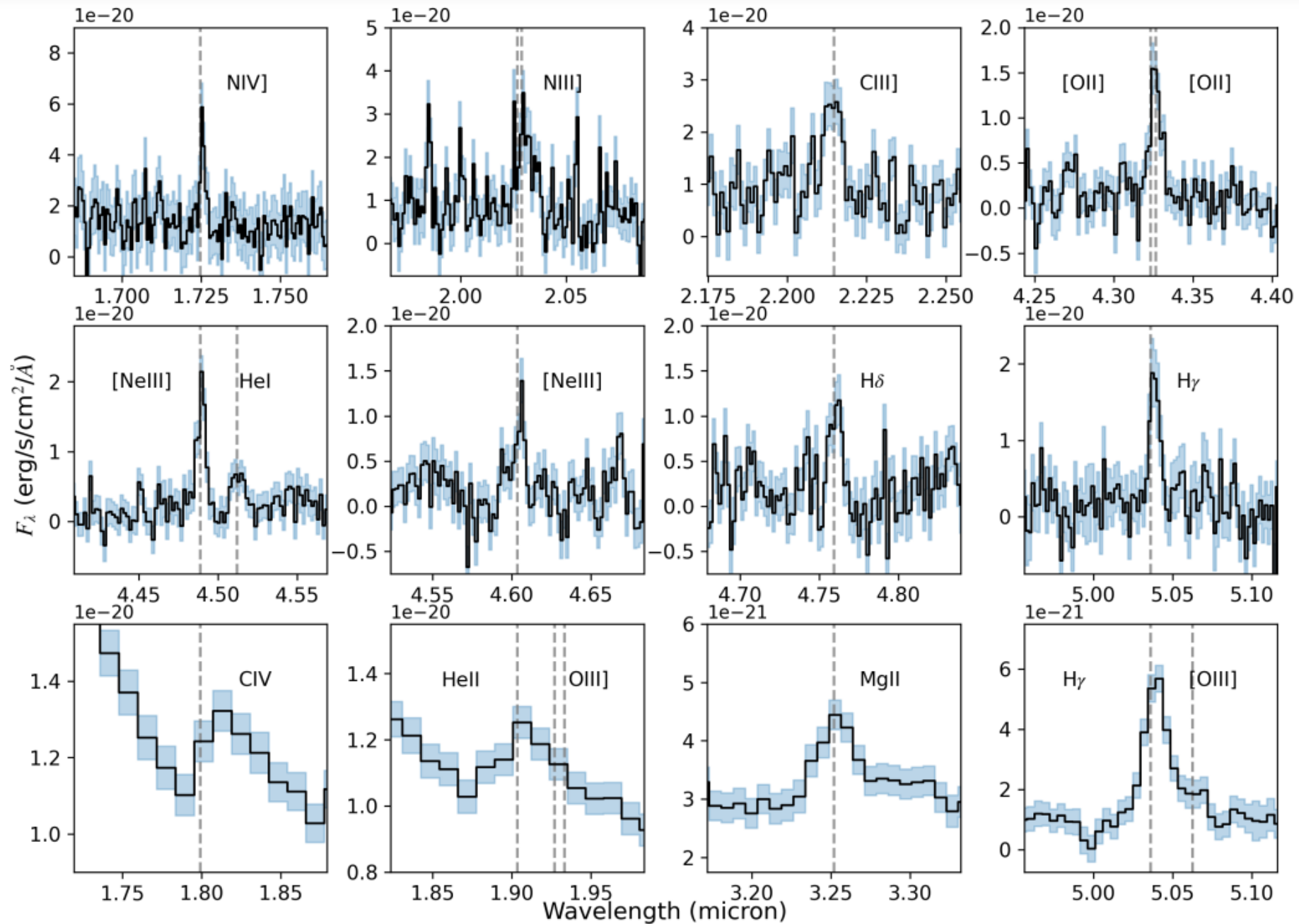


**Fig. 2.** Emission lines seen in GN-z11 from the Medium resolution gratings, apart from the last row that shows line emission from the low resolution prism spectrum. The C IV, He II+O III] Mg II and [O III]  $\lambda$ 4363 lines are not detected with high significance in the grating spectra.

# Как определили расстояние

- In determining the redshift from the vacuum rest-frame wavelengths, we exclude Lyman- $\alpha$  (which has a velocity offset, see Section 3.3) and also Mg ii (which is only significantly detected in the low-resolution prism), and do a weighted fit of 9 well-detected emission lines to give a redshift  $z = 10.6034 \pm 0.0013$ .



# Is GN-z11 an AGN?

- In a companion paper, Tacchella et al. (2023) analyze JADES NIRCcam imaging data and derive the best size constraint so far, finding an intrinsic half-light radius of only  $0.016 \pm 0.00500$  ( $64 \pm 20$  pc).
- N iv]  $\lambda 1486$  line (ionization potential  $E > 47.5$  eV) is often a signature of an AGN
- the higher ionization Nitrogen line N v ( $E > 77.5$  eV), which is a clear signature of AGN activity, is not detected in either the grating or the prism spectra
- we find that photoionization by an AGN is not favoured, and star formation alone may be able to explain the observed line ratios

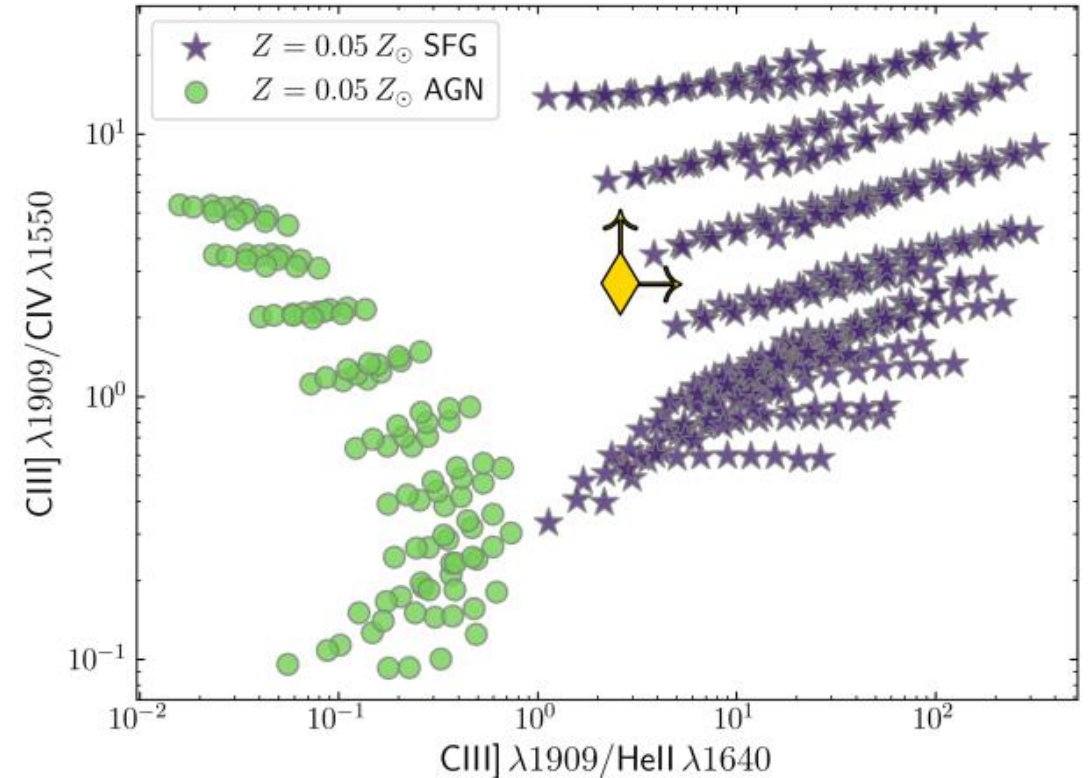


**Fig. 3.** Limits measured on C III]/He II vs C III]/C IV ratios for GN-z11 shown along with predictions from photoionization due to AGN (stars) and star-formation (circles) from [Feltre et al. \(2016\)](#) at a fiducial metallicity of  $Z = 0.05 Z_{\odot}$ . Based on the line ratios shown, photoionization due to an AGN is unlikely, with the limits favoring star-formation. We note that the parameter space probed by predictions for AGN and star-forming galaxies at different metallicities are similarly well separated.

- In the 2D spectrum of Figure 5 it is apparent that the Lyman $\alpha$  emission is more spatially extended than the continuum. Whilst the continuum flux is largely contained within 2 pixels (0.200), as expected based on the small size measured in our NIRC*am* imaging presented in Tacchella et al. (2023), the Lyman- $\alpha$  emission extends further to the south-west. The Lyman- $\alpha$  extension beyond the continuum is at least 2 pixels, corresponding to an extra 0.8 kpc
- The fact that Lyman- $\alpha$  is spatially extended is a remarkable result, which may be suggestive of a Lyman- $\alpha$  halo. The presence of such haloes around individual star-forming galaxies has been reported at lower redshifts (e.g. Rauch et al. 2008; Wisotzki et al. 2016; Leclercq et al. 2017; Kusakabe et al. 2022) and we may be seeing the gas in the circum-galactic medium (CGM), from Lyman- $\alpha$  fluorescence or shock heating.
- Large velocity offsets are key to the escape of Lyman- $\alpha$  photons from galaxies in a highly-neutral IGM. Since the damping wing of the IGM and proximate HI will absorb photons close to the resonant frequency, photons that escape must resonantly scatter in the wings. Those that scatter far enough to the red may then be able to escape the system without being absorbed



- The NIRSPEC spectrum of GN-z11 is remarkably rich with emission lines, enabling us to study the ISM properties at  $z > 10$ . Based on the high  $[\text{Ne III}]/[\text{O II}]$  ratio we infer a high ionization parameter ( $\log(U) > -2.0$ ). We report a significant detection of the very rarely-seen  $\text{N III} \lambda 1748$  line, which could suggest unusually high N/O ratios. While some high ionization lines are detected, the  $\text{He II} \lambda 1640$  and  $\text{C IV} \lambda 1550$  lines, which are typically associated with photoionization due to AGN, are weak. If this galaxy is indeed powered by star formation, then the Balmer emission lines and UV continuum suggest a current star formation rate of  $\sim 30 M_{\odot} \text{ yr}^{-1}$  and low dust attenuation.

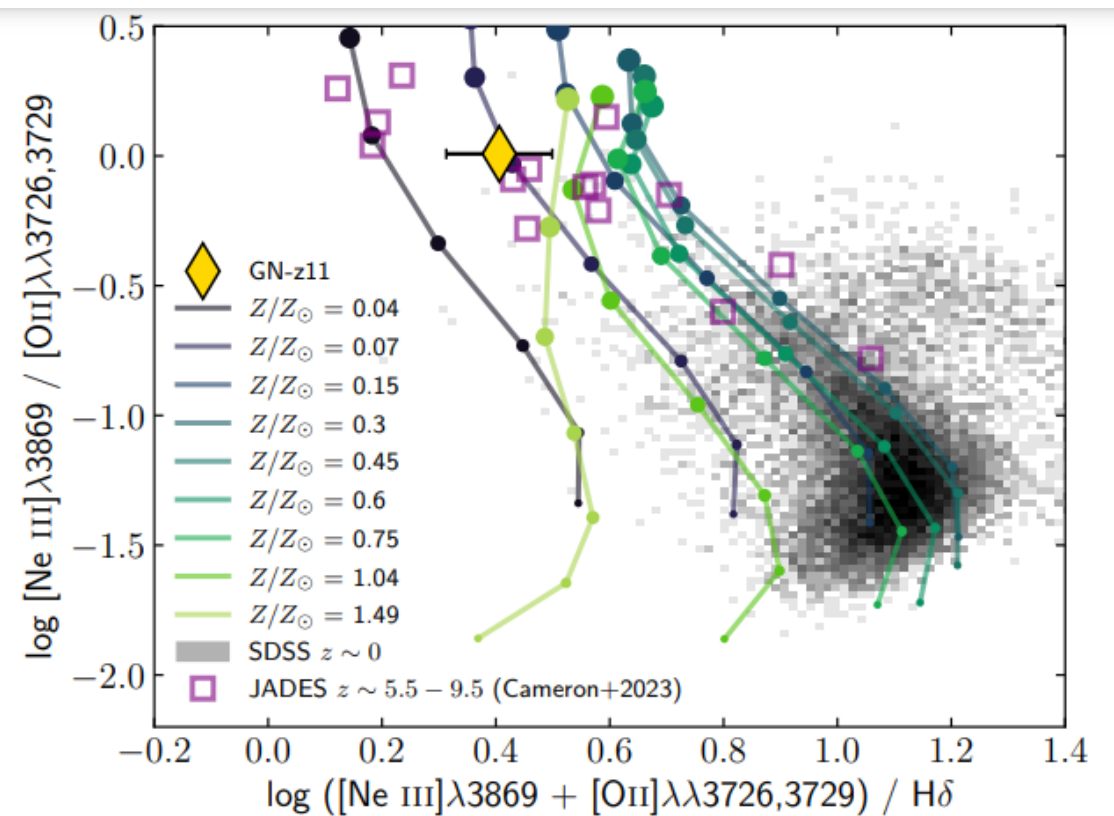


**Fig. 7.** Line ratio diagram, showing  $([\text{Ne III}] + [\text{O II}])/H\delta$  vs.  $[\text{Ne III}]/[\text{O II}]$ , featuring GN-z11 (yellow diamond). The background grey 2D PDF shows the subset of SDSS galaxies with  $0.03 < z < 0.1$  for which  $[\text{Ne III}]\lambda 3869$ ,  $[\text{O II}]\lambda\lambda 3726, 3729$  and  $H\delta$  are all detected with  $S/N > 5$ . Purple squares show  $z > 5.5$  galaxies from Cameron et al. (2023) after adjusting the reported ratios to be in terms of  $H\delta$  by assuming a fixed value of  $H\delta/H\beta = 0.268$ . Solid lines show model grids from Gutkin et al. (2016), plotted for nine different values of metallicity ( $Z/Z_{\odot} = 0.04, 0.07, 0.15, 0.30, 0.45, 0.60, 0.75, 1.0, 1.5$ ) indicated by the different colours, and seven values of ionization parameter, indicated by marker sizes, in steps of 0.5 from  $\log U = -4.0$  (smallest) to  $\log U = -1.0$  (largest).

# Nitrogen enhancements 440 Myr after the Big Bang: super-solar N/O, a tidal disruption event or a dense stellar cluster in GN-z11?

Alex J. Cameron,<sup>1</sup>★ Harley Katz<sup>1</sup>, Martin P. Rey<sup>1</sup> and Aayush Saxena<sup>1,2</sup>

<sup>1</sup>*Department of Physics, University of Oxford, Denys Wilkinson Building, Keble Road, Oxford, OX1 3RH, UK*

<sup>2</sup>*Department of Physics and Astronomy, University College London, Gower Street, London WC1E 6BT, UK*

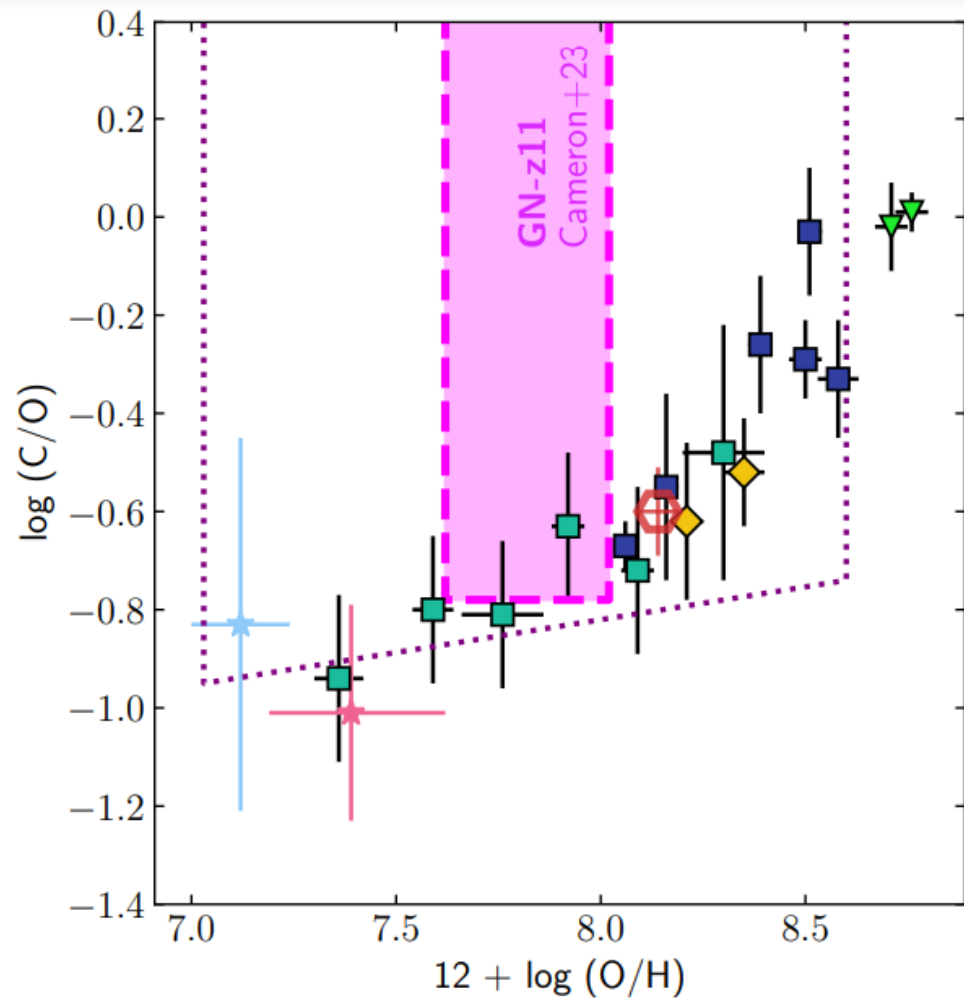
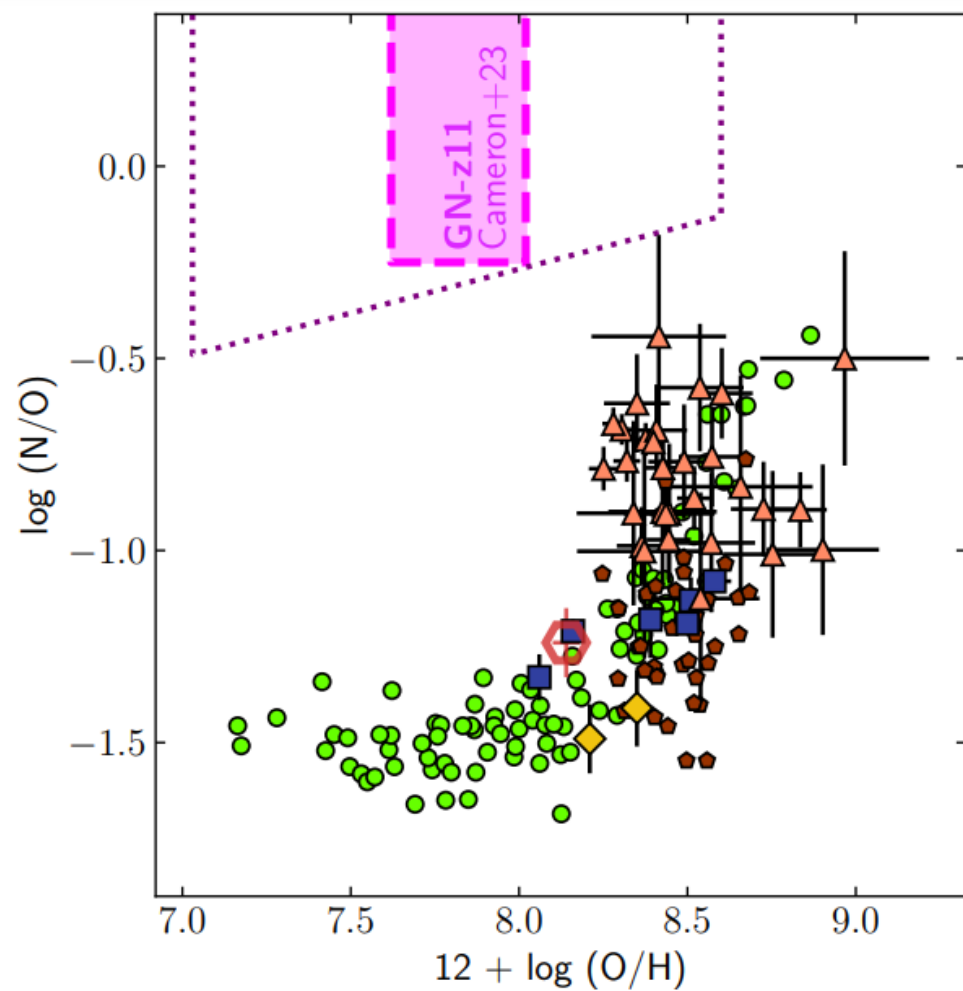
$\log(\text{N/O}) > -0.25$ , greater than four times solar

Abundance ratio	Fiducial	Conservative
$\log(\text{N/O})$	$> -0.25$	$> -0.49$
$\log(\text{C/O})$	$> -0.78$	$> -0.95$
$12 + \log(\text{O/H})$	7.82	$< 8.6$

**Table 1.** Summary of the abundance limits derived in Section 2. The ‘fiducial’ column takes its values from the  $T_e = 1.46 \times 10^4$  K column of Table A1. The N/O and C/O ratios in the ‘conservative’ column are the lowest values obtained from any combination of assumptions in Table A1, excluding the strongly disfavoured  $T_e = 3 \times 10^4$  K. The ‘conservative’ O/H value adopts the highest O/H value from Table A1 as an upper limit. Note that O/H abundance ratios are much more sensitive to modelling assumptions than metal abundance ratios. For reference, solar values are:  $\log(\text{N/O})_\odot = -0.86$ ,  $\log(\text{C/O})_\odot = -0.26$ ,  $12 + \log(\text{O/H})_\odot = 8.69$  (Asplund et al. 2009).

# Методы

- Emissivity calculations in this section are performed with pyneb (Luridiana et al. 2015), using the atomic data from the chianti database (version 10.0.2; Dere et al. 1997; Del Zanna et al. 2021). Emission lines fluxes used in these calculations are taken from Table 1 in B23, adopting measurements from their medium-resolution grating spectra.
- Because [O iii]  $\lambda$ 5007 is beyond the wavelength coverage of NIRSpec at  $z = 10.6$ , we first use O iii]  $\lambda\lambda$ 1660, 1666 along with [O iii]  $\lambda$ 4363 to derive an electron temperature constraint. If we assume that there is no dust reddening in the system (consistent with the  $H\delta/H\gamma$  ratio reported), the  $2\sigma$  upper limit on the O iii]  $\lambda\lambda$ 1660,1666/[O iii]  $\lambda$  4363 ratio ( $< 1.57$ ) gives us an upper limit on the temperature of  $< 1.25 \times 10^4$  K. This value is lower than previous electron temperature measurements at this epoch
- We consider an alternative approach for estimating the electron temperature, making use of the [O iii]  $\lambda$ 4363/[Ne iii]  $\lambda$ 3869 ratio. Neon and oxygen are both  $\alpha$ -elements and the Ne/O abundance ratio has been observed to be quite consistent across a large range of abundances and redshifts (e.g. Berg et al. 2019b, 2020; ArellanoCórdova et al. 2022). Furthermore, Ne<sup>++</sup> traces a similar ionisation zone to O<sup>++</sup>, meaning that [Ne iii]  $\lambda$ 3869 / [O iii]  $\lambda$ 5007 flux ratios typically do not show large variations (e.g. Witstok et al. 2021). Thus, we solve for the temperature at which the measured [O iii]  $\lambda$ 4363 / [Ne iii]  $\lambda$ 3869 flux ratio reproduces the solar Ne/O abundance ratio. This results in a temperature of  $T_e = 1.46 \pm 0.26 \times 10^4$  K, which is in reasonable agreement with the temperature limit inferred from the O iii]  $\lambda\lambda$ 1660,1666/[O iii]  $\lambda$ 4363 ratio.



- |   |  |  |
|---|--|--|
| <span style="color: magenta;">---</span> GN-z11: Fiducial               | <span style="color: blue;">■</span> Garnett+ 1999 ( $z \sim 0$ )   | <span style="color: cyan;">■</span> Garnett+ 1995 ( $z \sim 0$ )           |
| <span style="color: purple;">⋯</span> GN-z11: Conservative              | <span style="color: yellow;">◆</span> Esteban+ 2014 ( $z \sim 0$ ) | <span style="color: green;">▼</span> García-Rojas+ 2007 ( $z \sim 0$ )     |
| <span style="color: green;">●</span> Pilyugin+ 2012 ( $z \sim 0$ )      | <span style="color: brown;">▲</span> Berg+ 2020 ( $z \sim 0$ )     | <span style="color: red;">★</span> Jones+ 2023 ( $z = 6.229$ )             |
| <span style="color: brown;">◆</span> Hayden-Pawson+ 2022 ( $z \sim 2$ ) | <span style="color: red;">⊕</span> Steidel+ 2016 ( $z \sim 2.4$ )  | <span style="color: blue;">★</span> Arellano-Córdova+ 2022 ( $z = 8.495$ ) |

# Выводы

- We explore how our derived values vary with different assumptions of temperature, density, dust, and ionisation corrections, finding that none of these can reasonably explain the high N iii]  $\lambda 1750$  / O iii]  $\lambda\lambda 1660, 1666$  ratio without invoking a high N/O ratio. Given the longer enrichment timescales typically associated with nitrogen compared to oxygen, this over-enrichment is highly unexpected and seemingly at odds with the young age of the Universe at  $z = 10.6$
- We review whether the emission pattern observed in GNz11 could be powered by an AGN, disfavoured in B23, but which could bias the inferred N/O. We find qualitative parallels between this object and the population of rare 'nitrogen-loud' quasars, although emission line ratios observed in GNz11 would put it as an outlier of this already rare population.
- Assuming instead that GN-z11 is indeed a star-forming galaxy, as preferred by B23, we then review stellar processes that could produce high N/O at such early cosmic times. Traditional models of nitrogen-enrichment from AGB winds would likely require a highly contrived formation scenario, which cannot be ruled out but requires extensive validation against quantitative galactic enrichment models. Similarly, metal yields from exotic stellar evolution channels, including rotating and Pop. III massive stars, generally disfavour high nitrogen-to-oxygen production. Individual progenitor models can lead to high N/O, but generalizing across the galaxy would require an extremely finely-tuned progenitor mass function and initial conditions
- Lastly, we explore whether exotic dynamical mechanisms operating at high redshift could explain the apparent nitrogen-enhancement in GN-z11. Runaway stellar collisions in the cores of dense, high-redshift stellar clusters can lead to the formation of very massive stars, leading to rapid and abundant nitrogen production and an underproduction of oxygen. There are large quantitative uncertainties with this scenario, but it provides an avenue to simultaneously explain the high N/O in GN-z11 and the lack of low-redshift counterparts where gas densities become lower. These same star clusters would also be ideal sites to host TDEs which could also